Shear flow in smectic A liquid crystals

2009 J. Phys.: Condens. Matter 21 465101

(http://iopscience.iop.org/0953-8984/21/46/465101)

J. Phys.: Condens. Matter **21** (2009) 465101 (13pp) doi:10.1088/0953-8984/21/46/465101

Shear flow in smectic A liquid crystals

I W Stewart[1] **and F Stewart**

Department of Mathematics, University of Strathclyde, Livingstone Tower, 26 Richmond Street, Glasgow G1 1XH, UK

E-mail: i.w.stewart@strath.ac.uk

Received 18 June 2009, in final form 2 September 2009
Published 26 October 2009
Online at stacks.iop.org/JPhysCM/21/465101

Abstract

This paper considers the onset of a shear-induced instability in a sample of smectic A liquid crystal. Unlike many previous models, the usual director **n** need not necessarily coincide with the local smectic layer normal **a**; the traditional Oseen constraint ($\nabla \times \mathbf{a} = \mathbf{0}$) is not imposed when flow is present. A recent dynamic theory for smectic A (Stewart 2007 *Contin. Mech. Thermodyn.* **18** 343–60) will be used to examine a stationary instability in a simple model when the director reorientation and smectic layer distortions are, firstly, assumed not to be coupled to the velocity and, secondly, are supposed coupled to the velocity. A critical shear rate at which the onset of the instability occurs will be identified, together with an accompanying critical director tilt angle and critical wavenumber for the associated smectic layer undulations. Despite some critical phenomena being largely unaffected by any coupling to the flow, it will be shown that the influence of some material parameters, especially the smectic layer compression constant B_0 and the coupling constant B_1, upon the critical shear rate and critical tilt angle can be greatly affected by flow.

1. Introduction

Liquid crystals are anisotropic fluids that consist of elongated rod-like molecules which have a preferred local average orientation described by the unit vector **n**, commonly called the director. In the smectic A (SmA) liquid crystal phase the molecules are arranged in equidistant layers where, in general, the director is often parallel to the local smectic layer normal, denoted by the unit vector **a**, as shown in figure 1(a). It is well known that the orientations of **n** and **a** can be affected by an imposed shear flow, boundary conditions or an externally applied electric or magnetic field. This paper will deal with the analysis of a simple shear applied to a planar aligned sample of SmA. At a critical shear rate the director and the smectic layers will adjust their alignment through undulations of the layers and realignment of the director relative to the layers. This critical shear rate turns out to be directly related to the critical angle, measured relative to the initial unperturbed layer normal direction, at which the director will tilt at the onset of a shear-induced flow instability. The main aim is to identify the critical share rate, k_c, the critical director tilt angle, θ_c, and the accompanying critical wavenumber, q_c, that signals the presence of the undulations in the smectic layers. The critical wavevector for these undulations is perpendicular to the direction of the applied shear, in accordance with related experimental and theoretical results that are mentioned below. More general details on the physics and mathematical models of liquid crystals can be found in the books by de Gennes and Prost [1] and Stewart [2].

In the classical models for SmA, the director **n** and smectic layer normal **a** coincide [1, 2]. However, the investigations by Ribotta and Durand [3], Oswald and Ben-Abraham [4] and, more recently, Auernhammer *et al* [5–7], Soddemann *et al* [8] and Stewart *et al* [9–11] have indicated a need for a model that allows **n** and **a** to separate if required. The possibility of introducing such a separation has been discussed by these authors and a nonlinear continuum theory that takes this separation into account for the dynamics of SmA has been formulated by Stewart [12]. It is this continuum theory that will be employed here while the approach we adopt will follow that of Auernhammer *et al* [6]. We consider a simple shear imposed upon an initially planar aligned sample of SmA as shown in figure 1(b), which is motivated by the work in [4–6]. The results in [6], achieved using an alternative mathematical framework, can be compared qualitatively with those that will be featured here. It will be seen that, for the 'minimal' set of variables case discussed below when it is supposed that there is no coupling to the velocity field, the linear equations used in [6] coincide with those obtained here, as may be expected when a basic viscous stress is considered and the linearized

[1] Author to whom any correspondence should be addressed.

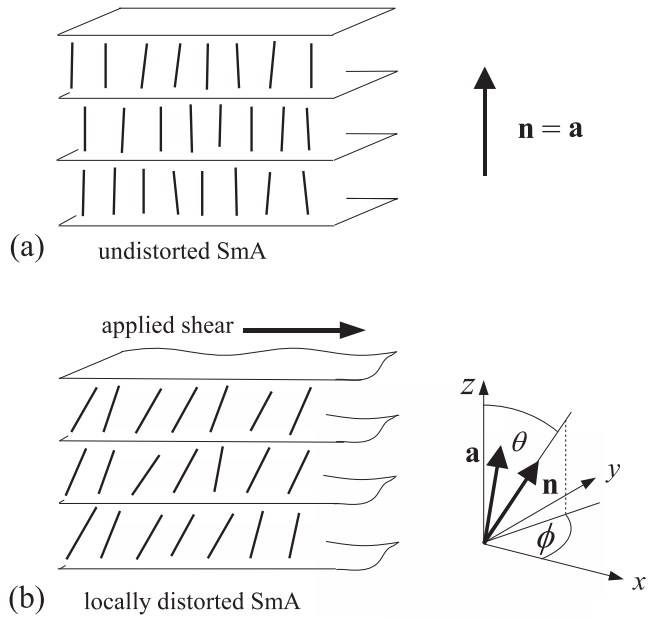

Figure 1. (a) A planar aligned sample of undistorted SmA liquid crystal. The short bold lines, which represent the director, are representative of the rod-like molecular structures within the layers. In this case the director **n** coincides with the layer normal **a**. (b) Subject to horizontal shear, the layers begin to distort and **n** and **a** need no longer coincide. The director is initially expected to tilt in the direction of flow while the wavevector, which is indicative of layer undulations, is parallel to the y axis. The angle θ measures the director tilt from the z axis and ϕ is the orientation angle of the orthogonal projection of **n** onto the smectic layers in the xy plane.

equations from the models are used. Nevertheless, when a full set of variables is used that couples to the velocity field, the linearized equations give some differing qualitative results due to the more extensive viscous stress terms that have been introduced in [12]. A comparison will be made between the solutions for critical parameters obtained from the minimal and full sets of variables. Some qualitative features will turn out to be modelled adequately by adopting the reduced minimal set of variables and this will be indicative of when a simplified set of model equations may be sufficient. On the other hand, there will be instances when the full influence of flow cannot be neglected because the results differ dramatically. In this case coupling to the flow profile cannot be ignored and a more complex set of model equations are required.

The dynamic theory for SmA will be summarized in section 2.1 and the mathematical model of the geometric set-up for a simple shear will be introduced in section 2.2. A spatially homogeneous state, previously identified in [6], will be presented briefly in section 2.3. This homogeneous state is important because it relates the shear rate to the director tilt angle. Section 3 considers small disturbances to the spatially homogeneous state and presents the main governing perturbation equations in two cases: the first ignores any coupling of the disturbances to the flow and the second includes the possibility of such coupling. Section 4 discusses the numerical results via various graphs for the identification of the critical parameters k_c, θ_c and q_c at the onset of an instability to the spatially homogeneous state. Comparisons will made between the results for the two sets of solutions and differences will be highlighted that will indicate when coupling to the flow may or may not be neglected for various ranges of material parameters. The paper closes in section 5 with a discussion of the results.

2. Dynamic equations and geometrical set-up

The SmA dynamic theory of Stewart [12], which allows **n** and **a** to separate, will be introduced in section 2.1 before going on to discuss the geometrical set-up and particular model equations in section 2.2.

2.1. Dynamic theory

The dynamic theory formulated in [12] will now be summarized. Cartesian tensor notation and the summation convention will be used, where any index that is repeated precisely twice in an expression is summed from 1 to 3. Partial differentiation with respect to the variable x_j is denoted by a subscript j preceded by a comma. For example, $a_{i,j}$ denotes the partial derivative of the ith component of **a** with respect to the jth spatial coordinate and $a_{i,i}$ represents the divergence of **a**. The layer normal **a** is given by

$$a_i = \frac{\Phi_{,i}}{|\nabla\Phi|}, \qquad a_i a_i = 1, \tag{2.1}$$

where the smectic layers are modelled by the layer function Φ. The usual Oseen [13] constraint, $\nabla \times \mathbf{a} = \mathbf{0}$, a condition that is widely accepted for modelling the equilibrium structures of layered smectic phases in the absence of dislocations, will not be imposed as a modelling requirement for the dynamics: small distortions to the lamellar-like layer structure of SmA generally violate the Oseen constraint. The director must satisfy the constraint

$$n_i n_i = 1. \tag{2.2}$$

The incompressibility condition is given by

$$v_{i,i} = 0, \tag{2.3}$$

where **v** is the velocity. The rate of strain tensor A and vorticity tensor W are second-order tensors defined in the usual way by

$$A_{ij} = \tfrac{1}{2}(v_{i,j} + v_{j,i}), \qquad W_{ij} = \tfrac{1}{2}(v_{i,j} - v_{j,i}), \tag{2.4}$$

and, following the standard procedure for nematics, the co-rotational time flux **N** of the director **n** is introduced as

$$\mathbf{N} = \dot{\mathbf{n}} - \mathsf{W}\mathbf{n}. \tag{2.5}$$

The equations that arise from the balance law for linear momentum are

$$\rho\dot{v}_i = \rho F_i - \tilde{p}_{,i} + \tilde{g}_j n_{j,i} + G_j n_{j,i} + |\nabla\Phi| a_i J_{j,j} + \tilde{t}_{ij,j}, \tag{2.6}$$

where ρ is the density, F_i is the external body force per unit mass, G_i is the generalized external body force that can be related to the external body moment per unit mass, $\tilde{p} = p + w_A$

where p is the pressure and w_A is the energy density, and $\mathbf{J}$ is defined by

$$J_i = -\frac{\partial w_A}{\partial\, \Phi_{,i}} + \frac{1}{|\nabla\Phi|}\left[\left(\frac{\partial w_A}{\partial a_{p,k}}\right)_{,k} - \frac{\partial w_A}{\partial a_p}\right](\delta_{pi} - a_p a_i). \quad (2.7)$$

A superposed dot represents the usual material time derivative given by

$$\frac{D}{Dt} = \frac{\partial}{\partial t} + v_i \frac{\partial}{\partial x_i}. \quad (2.8)$$

We remark here that $\mathbf{J}$, sometimes called a 'phase flux' term, is a natural nonlinear extension to the versions discussed by Auernhammer *et al* [5, 6], E [14] and de Gennes and Prost [1]: when it is suitably linearized for small changes in the layer and director orientations then it reduces to the expressions discussed in [5, 6] when $\mathbf{n}$ and $\mathbf{a}$ are allowed to separate and further reduces to the classical results in [1, 14] when $\mathbf{n} \equiv \mathbf{a}$. The constitutive equations for the viscous stress $\tilde{t}_{ij}$ and $\tilde{g}_i$ are given by, respectively,

$$\begin{aligned}\tilde{t}_{ij} &= \alpha_1(n_k A_{kp} n_p) n_i n_j + \alpha_2 N_i n_j + \alpha_3 n_i N_j + \alpha_4 A_{ij} \\ &\quad + \alpha_5(n_j A_{ip} n_p + n_i A_{jp} n_p) + (\alpha_2 + \alpha_3) n_i A_{jp} n_p \\ &\quad + \tau_1(a_k A_{kp} a_p) a_i a_j + \tau_2(a_i A_{jp} a_p + a_j A_{ip} a_p) \\ &\quad + \kappa_1(a_i N_j + a_j N_i + n_i A_{jp} a_p - n_j A_{ip} a_p) \\ &\quad + \kappa_2(n_k A_{kp} a_p)(n_i a_j + a_i n_j) \\ &\quad + \kappa_3[(n_k A_{kp} n_p) a_i a_j + (a_k A_{kp} a_p) n_i n_j] \\ &\quad + \kappa_4[2(n_k A_{kp} a_p) n_i n_j + (n_k A_{kp} n_p)(a_i n_j + n_i a_j)] \\ &\quad + \kappa_5[2(n_k A_{kp} a_p) a_i a_j + (a_k A_{kp} a_p)(n_i a_j + a_i n_j)] \\ &\quad + \kappa_6(n_j A_{ip} a_p + n_i A_{jp} a_p + a_i A_{jp} n_p + a_j A_{ip} n_p), \quad (2.9)\end{aligned}$$

and

$$\tilde{g}_i = -\gamma_1 N_i - \gamma_2 A_{ip} n_p - 2\kappa_1 A_{ip} a_p, \quad (2.10)$$

where

$$\gamma_1 = \alpha_3 - \alpha_2 \qquad \text{and} \qquad \gamma_2 = \alpha_2 + \alpha_3. \quad (2.11)$$

In the above expressions, α_1 to α_5, τ_1, τ_2 and κ_1 to κ_6 are dynamic viscosity coefficients. The viscosities α_1 to α_5 are nematic-like, while the three particular viscosities α_4, τ_1 and τ_2 are analogous to the usual incompressible SmA viscosities [14, equation (3.33)]; κ_1 to κ_6 are 'coupling' viscosities that reflect the combined effects of nematic and SmA behaviour. We remark here that Sukumaran and Ranganath [15] also have an expression for an analogous $\tilde{g}_i$ contribution for smectic C (SmC) liquid crystals that contains three viscosity coefficients similar in style to that stated in (2.10) and that a more extensive theory for SmC [16] has similar contributions.

The balance of angular momentum leads to the equations

$$\left(\frac{\partial w_A}{\partial n_{i,j}}\right)_{,j} - \frac{\partial w_A}{\partial n_i} + \tilde{g}_i + G_i = \mu n_i, \quad (2.12)$$

where the scalar function μ is a Lagrange multiplier that arises from the constraint (2.2) and can usually be eliminated from these equations or evaluated by taking the scalar product of (2.12) with $\mathbf{n}$. The permeation equation is

$$\dot{\Phi} = -\lambda_{\mathrm{p}} J_{i,i}, \quad (2.13)$$

where $\lambda_{\mathrm{p}} \geqslant 0$ is the permeation coefficient, which relates the layer flux through a stationary medium to the relevant thermodynamic force [1, 17]. In locally planar smectic systems, permeation can be thought of as a weak flow of material through the smectic layers in the direction of the local layer normal [18]. It was first introduced by Helfrich [19]. Equations (2.2), (2.3), (2.6), (2.12) and (2.13) provide nine equations in the nine unknowns Φ, n_i, v_i, p and μ; the smectic layer normal $\mathbf{a}$ is, of course, determined by (2.1) from the solution for Φ.

One elementary possibility for an energy density may be based upon those used by Ribotta and Durand [3], E [14], Auernhammer *et al* [5, 6] and Soddemann *et al* [8]. It is given by [12]

$$\begin{aligned}w_A &= \tfrac{1}{2}K_1^n(\nabla\cdot\mathbf{n})^2 + \tfrac{1}{2}K_1^a(\nabla\cdot\mathbf{a})^2 \\ &\quad + \tfrac{1}{2}B_0(|\nabla\Phi| + \mathbf{n}\cdot\mathbf{a} - 2)^2 + \tfrac{1}{2}B_1\left\{1 - (\mathbf{n}\cdot\mathbf{a})^2\right\}. \quad (2.14)\end{aligned}$$

This energy density is invariant under the simultaneous changes in sign $\mathbf{n} \to -\mathbf{n}$ and $\mathbf{a} \to -\mathbf{a}$, which is equivalent to invariance under the simultaneous changes $\mathbf{n} \to -\mathbf{n}$ and $\nabla\Phi \to -\nabla\Phi$. The first term on the right-hand side of (2.14) represents the usual elastic splay deformation of the director $\mathbf{n}$ while the second term is a measure of the bending of the smectic layers; both K_1^n and K_1^a are positive elastic constants. The third term represents smectic layer compression and is an extended version of that which is known for SmA, based upon the results in [1, 6, 14]; the positive constant B_0 is the layer compression constant. The fourth expression is a measure of the strength of the coupling between $\mathbf{n}$ and $\mathbf{a}$ with the positive constant B_1 having dimensions of energy per unit volume: in an equilibrium state this energy contribution is clearly minimized when $\mathbf{n}$ and $\mathbf{a}$ are parallel. Since $\mathbf{n}$ and $\mathbf{a}$ are unit vectors, this term can equally be written as $\frac{1}{2}B_1(\mathbf{n}\times\mathbf{a})^2$, which is the form used in [5, 6, 8].

2.2. Geometrical set-up and approximations

We consider a homeotropically aligned sample of SmA liquid crystal subjected to a simple shear flow as shown in figure 1. It will be assumed that any undulations will be independent of x for small disturbances, in accord with the experimental interpretations of Oswald and Ben-Abraham [4] and the theoretical framework of Auernhammer *et al* [5, 6] and Soddemann *et al* [8]: there will be a wavevector along the y direction while the basic shear velocity will be along the x direction for a shear-induced flow imposed upon the layers as indicated in figure 1(b). The general form for the layer function Φ may then be written as

$$\Phi = z - u(y, z, t), \quad (2.15)$$

where u is the smectic layer displacement.

It is generally possible to set

$$\mathbf{n} = (\sin\theta\cos\phi, \sin\theta\sin\phi, \cos\theta), \quad (2.16)$$

$$\mathbf{a} = \frac{\nabla\Phi}{|\nabla\Phi|}, \quad (2.17)$$

where $\theta(y, z, t)$ is the angle between $\mathbf{n}$ and the z axis and $\phi(y, z, t)$ is the angle measured relative to the x axis that is made by the orthogonal projection of $\mathbf{n}$ onto the xy plane. In general, the layer function Φ is to be determined. As noted in [6], for small disturbances to the director and layer structure we expect the difference between the director splay deformation and the bending of the layers to be negligible. We therefore combine the corresponding energy contributions into a single term with the new elastic constant K (which will be of the same order as K_1^n or K_1^a) defined through the approximation

$$\tfrac{1}{2}K_1^n(\nabla\cdot\mathbf{n})^2 + \tfrac{1}{2}K_1^a(\nabla\cdot\mathbf{a})^2 \approx \tfrac{1}{2}K(\nabla\cdot\mathbf{a})^2. \tag{2.18}$$

In an initial investigation, such as this, the viscous stress $\tilde{t}_{ij}$ may be simplified so that calculations can be related to results in the context of related nematic and smectic theories. We therefore decide to neglect all 'coupling' viscosities κ_1 to κ_6, so that seven viscosity coefficients remain: α_1 to α_5, τ_1 and τ_2. These are the principal nematic-like and smectic-like viscosities. The incorporation of the κ_i viscosities will be the subject of future more extensive work. The external body force $\mathbf{F}$ and generalized external body force $\mathbf{G}$ will be neglected. The bulk energy density w_A, viscous stress $\tilde{t}_{ij}$ and $\tilde{g}_i$ that will be considered in the current model are therefore, using (2.14), (2.9) and (2.10), respectively,

$$\begin{aligned} w_A &= \tfrac{1}{2}K(\nabla\cdot\mathbf{a})^2 + \tfrac{1}{2}B_0(|\nabla\Phi| + \mathbf{n}\cdot\mathbf{a} - 2)^2 \\ &\quad + \tfrac{1}{2}B_1\{1-(\mathbf{n}\cdot\mathbf{a})^2\}, \end{aligned} \tag{2.19}$$

$$\begin{aligned} \tilde{t}_{ij} &= \alpha_1(n_kA_{kp}n_p)n_in_j + \alpha_2N_in_j + \alpha_3n_iN_j + \alpha_4A_{ij} \\ &\quad + \alpha_5(n_jA_{ip}n_p + n_iA_{jp}n_p) + (\alpha_2+\alpha_3)n_iA_{jp}n_p \\ &\quad + \tau_1(a_kA_{kp}a_p)a_ia_j + \tau_2(a_iA_{jp}a_p + a_jA_{ip}a_p), \end{aligned} \tag{2.20}$$

$$\tilde{g}_i = -\gamma_1N_i - \gamma_2A_{ip}n_p. \tag{2.21}$$

A spatially homogeneous state under simple shear will now be identified using the theory and approximations outlined above. Disturbances to this homogeneous state will then form the core of the work to be carried out in sections 3 and 4.

2.3. A spatially homogeneous state

The starting point for our investigation is the identification of a spatially homogeneous alignment under a simple shear. Following the approach of Auernhammer *et al* [6] and Soddemann *et al* [8], it will assumed that, within such a spatially homogeneous state, distortions to the smectic layer alignment are negligible (this will, of course, not be the case when we investigate disturbances to such a state). It is also supposed that the director tilts relative to the smectic layer normal but does not twist out of the xz plane in a first approximation. Thus to determine a spatially homogeneous state we set

$$\Phi = z, \qquad \phi = 0, \qquad \theta = \theta_0, \tag{2.22}$$

where θ_0 is some constant angle. The form for the director $\mathbf{n}$ and layer normal $\mathbf{a}$ are therefore given via (2.16) and (2.17) by

$$\mathbf{a} = (0, 0, 1) \qquad \text{and} \qquad \mathbf{n} = (\sin\theta_0, 0, \cos\theta_0). \tag{2.23}$$

For the associated simple shear it is assumed that the velocity has the form

$$\mathbf{v} = (kz, 0, 0), \tag{2.24}$$

where $k > 0$ is the shear rate, motivated by figure 1(b). The constraints (2.1) and (2.2) are clearly satisfied and the incompressibility condition (2.3) is fulfilled. It is also evident that the permeation equation (2.13) is automatically satisfied. In the absence of external body forces it is easily verified that the linear momentum equations (2.6) reduce to $\tilde{p}_i = 0$, so that these equations are satisfied by setting $\tilde{p} = p + w_A$ to an arbitrary constant. The only remaining equations to be solved arise from the angular momentum equations (2.12) which, in this case, reduce to

$$-\frac{\partial w_A}{\partial n_i} + \tilde{g}_i = \mu n_i, \tag{2.25}$$

where w_A and $\tilde{g}_i$ are given by (2.19) and (2.20), respectively. Calculations reveal that (2.25) becomes

$$[B_1\cos\theta_0 + B_0(1-\cos\theta_0)]a_i + \tilde{g}_i = \mu n_i, \tag{2.26}$$

where

$$\begin{aligned} \tilde{g}_1 &= \tfrac{1}{2}k(\gamma_1-\gamma_2)\cos\theta_0, \qquad \tilde{g}_2 = 0, \\ \tilde{g}_3 &= -\tfrac{1}{2}k(\gamma_1+\gamma_2)\sin\theta_0. \end{aligned} \tag{2.27}$$

It is clear that for $i = 2$ equation (2.26) is satisfied identically. The Lagrange multiplier μ can be eliminated by subtracting the equations that result from multiplying the $i = 1$ equation by $\cos\theta_0$ and the $i = 3$ equation by $\sin\theta_0$ to show that the angular momentum equations finally reduce to the single equation

$$\begin{aligned} k\left[\frac{1+\lambda}{2} - \lambda\sin^2(\theta_0)\right] &= \frac{B_1}{\gamma_1}\sin(\theta_0)\cos(\theta_0) \\ &\quad + \frac{B_0}{\gamma_1}\sin(\theta_0)(1-\cos(\theta_0)), \end{aligned} \tag{2.28}$$

where $\lambda = -\gamma_2/\gamma_1$ is the dimensionless flow-alignment parameter (usually of order unity in many nematics [20]). Thus we have generated a well-defined relationship between the shear rate, k, and the tilt angle of the director, θ_0; this is in accord with the result determined by Auernhammer *et al* [6, equation (38)]. The relation (2.28) is of crucial importance when evaluating expressions below because it allows us to interchange the roles of θ_0 and k.

If we now consider (2.28) for small θ_0 it is seen that

$$\theta_0 = \frac{\gamma_1}{B_1}k\left(\frac{1+\lambda}{2}\right) + O(\theta_0^2), \tag{2.29}$$

a result observed previously [6]. Equation (2.29), to lowest order, gives an approximation for the tilt angle θ_0 in terms of the shear rate k, where θ_0 is seen to depend linearly upon k. Furthermore, this result is significant because it also shows that initially the dependence of θ_0 varies inversely with the coupling term B_1. As B_1 increases, the director $\mathbf{n}$ attempts to align along the direction of the layer normal $\mathbf{a}$ because the tilt angle θ_0 will correspondingly decrease. This is perhaps as expected since an increase in the magnitude of the coupling constant should

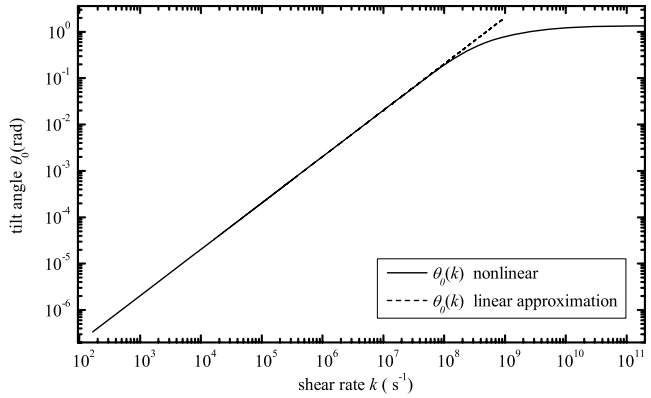

Figure 2. The dependence of θ_0 upon the shear rate k plotted on a log–log graph for the values of B_0, B_1, γ_1 and γ_2 in table 1. The solid curve has been obtained from the nonlinear relation (2.28) and the dashed curve is the linear approximation obtained from (2.29).

lead to a reduced separation in the angle between **n** and **a**. The angle θ_0 can be observed in a simple shear experiment at a given shear rate k. If the viscosities γ_1 and γ_2 are known, or can be estimated, then the relation (2.29) allows an estimate to be made for the constant B_1. If B_0 is also known then (2.28) provides a more accurate measurement of B_1. Figure 2 shows the dependence of θ_0 upon k for the results in (2.28) and (2.29) for the typical values of B_0, B_1, γ_1 and γ_2 stated in table 1 below.

We now go on to investigate the stability of the spatially homogeneous state identified above in two cases. The first case will assume that the flow induced by the shear does not couple to any perturbations to the variables that model **n** and **a** while the second case does suppose that the flow influences them and vice versa.

3. Stationary instability

This section considers small disturbances to the spatially homogeneous state (2.22) when perturbations are introduced to the director tilt θ, director twist ϕ, smectic layer function Φ and the induced shear flow $\mathbf{v} = (kz, 0, 0)$. Two cases will be considered. In the first case, in section 3.1, we shall ignore any coupling of this induced velocity to perturbations of the first three of the above variables. This preliminary approximation will be shown to be justified for a wide range of values of the elastic constants and compression modulus. This will be evident when we discuss the dynamic equations for the second case in section 3.2 when coupling of the director and layer normal to a perturbation of the velocity field will also be included. It is well known that there can be intricate coupling between flow and director alignment in nematic liquid crystals and this motivates an investigation into the more complex case of flow coupled to the perturbations of **n** and **a**. The objective is to determine a critical director tilt θ_c (which is related to a critical shear rate k_c through (2.28)) and associated critical wavenumber q_c at which the spatially homogeneous state identified in section 2 will exhibit the onset of undulating smectic layers possessing an identifiable wavelength equal to $2\pi/q_c$. The basic equations for the two cases will be derived in this section and numerical calculations will be presented in section 4.

Table 1. Typical material parameters discussed in the text.

Parameter	Typical value
d	10^{-5} m
q_z	π/d
K	5×10^{-12} N
B_0	8.95×10^{7} N m^{-2}
B_1	4×10^{7} N m^{-2}
λ_p	10^{-16} m^2 Pa^{-1} s^{-1}
α_1	-0.0060 Pa s
α_2	-0.0812 Pa s
α_3	-0.0036 Pa s
α_4, τ_1, τ_2	0.0652 Pa s
α_5	0.0640 Pa s
$\gamma_1 = \alpha_3 - \alpha_2$	0.0776 Pa s
$\gamma_2 = \alpha_2 + \alpha_3$	-0.0848 Pa s
ρ	1000 kg m^{-3}

3.1. Case 1: coupling to the velocity ignored

In the first instance, consider a perturbation to the spatially homogeneous simple shear problem in section 2.3 without any coupling to the induced flow, that is, the velocity for the homogeneous alignment is unperturbed while θ_0, ϕ and Φ are perturbed. Consider perturbations to (2.22) of the form

$$\Phi = z - \hat{u}(y, z), \qquad \phi = \hat{\phi}(y, z), \qquad \theta = \theta_0 + \hat{\theta}(y, z), \tag{3.1}$$

where $\hat{\theta}$, $\hat{u}$ and $\hat{\phi}$ are small with $\mathbf{v} = (kz, 0, 0,)$ where k can be replaced when required by an equivalent expression in θ_0 via the relation (2.28). We shall refer to the set of three variables $\hat{\theta}$, $\hat{u}$ and $\hat{\phi}$ as the minimal set of variables. Partial differentiation with respect to a spatial variable will be denoted by a corresponding subscript preceded by a comma. We can linearize in these variables to find that, to first order, with **n** given via (2.16):

$$\nabla\Phi = (0, -\hat{u}_{,y}, 1 - \hat{u}_{,z}), \qquad |\nabla\Phi| = 1 - \hat{u}_{,z}, \tag{3.2}$$

$$\mathbf{a} = (0, -\hat{u}_{,y}, 1),$$
$$\mathbf{n} = (\sin\theta_0 + \hat{\theta}\cos\theta_0, \hat{\phi}\sin\theta_0, \cos\theta_0 - \hat{\theta}\sin\theta_0), \tag{3.3}$$

and therefore the constraints (2.1) and (2.2) are satisfied to first order. The incompressibility condition (2.3) remains valid here also. As is common in similar problems [2, p 315], [6], the linear momentum equations may be ignored when using the minimal set of variables. In other words, neglecting equations (2.6) is often considered a good approximation when working with a minimal set of variables that are not coupled to the flow. How accurate this approximation is will become clear when a coupling of the minimal set to the flow is made in section 3.2 (to be mathematically consistent, coupling to the flow must be considered). The remaining equations to be solved are therefore those arising from angular momentum in equation (2.12) and the permeation equation (2.13), which we now consider. This will result in three governing equations for the perturbations.

The $\tilde{g}_i$ contributions, from (2.21), are

$$\tilde{g}_1 = \tfrac{1}{2}k(\gamma_1 - \gamma_2)(\cos\theta_0 - \hat{\theta}\sin\theta_0), \qquad \tilde{g}_2 = 0, \qquad \tilde{g}_3 = -\tfrac{1}{2}k(\gamma_1 + \gamma_2)(\sin\theta_0 + \hat{\theta}\cos\theta_0). \tag{3.4}$$

Straightforward calculations show that (2.12) becomes

$$B_1(\mathbf{n}\cdot\mathbf{a})a_i - B_0(|\nabla\Phi| + \mathbf{n}\cdot\mathbf{a} - 2)a_i + \tilde{g}_i = \mu n_i, \tag{3.5}$$

which can be linearized to find that

$$B_1(\cos\theta_0 - \hat{\theta}\sin\theta_0)a_i - B_0(\cos\theta_0 - \hat{\theta}\sin\theta_0 - 1 - \hat{u}_{,z})a_i + \tilde{g}_i = \mu n_i. \tag{3.6}$$

The Lagrange multiplier μ may be obtained by taking the scalar product of (3.6) with $\mathbf{n}$, defined in (3.3). However, in this special case, it is seen that μ can be obtained directly from the equation for $i = 1$. Working to first order reveals that

$$\mu = \tfrac{1}{2}k(\gamma_1 - \gamma_2)(\cot\theta_0 - \hat{\theta}\mathrm{cosec}^2\theta_0). \tag{3.7}$$

Consequently, the $i = 1$ equation is satisfied for this value of μ. Inserting μ into the equations for $i = 2$ results in the equation

$$\frac{1}{\gamma_1}[B_1 + B_0(\sec\theta_0 - 1)]\hat{u}_{,y} + \frac{1}{2}k(1+\lambda)\hat{\phi} = 0 \tag{3.8}$$

recalling that $\lambda = -\gamma_2/\gamma_1$. Similarly, for $i = 3$ we have

$$\left[\frac{B_1}{\gamma_1}\sin\theta_0\cos\theta_0 + \frac{B_0}{\gamma_1}\sin\theta_0(1-\cos\theta_0) - k\left(\frac{1+\lambda}{2} - \lambda\sin^2\theta_0\right)\right] + \left[\frac{\sin^2\theta_0}{\gamma_1}(B_0 - B_1) + k\lambda\sin\theta_0\cos\theta_0 + \frac{k}{2}(1+\lambda)\cot\theta_0\right]\hat{\theta} + \frac{B_0}{\gamma_1}\hat{u}_{,z}\sin\theta_0 = 0. \tag{3.9}$$

The expression in the first pair of square brackets above is zero, by the relation (2.28), and so this equation further reduces to

$$\left[\frac{\sin^2\theta_0}{\gamma_1}(B_0 - B_1) + k\lambda\sin\theta_0\cos\theta_0 + \frac{k}{2}(1+\lambda)\cot\theta_0\right]\hat{\theta} + \frac{B_0}{\gamma_1}\hat{u}_{,z}\sin\theta_0 = 0. \tag{3.10}$$

After some algebraic manipulation, this particular equation can be shown to coincide with that of Auernhammer *et al* [6 equation (42)] if the relation (2.28) is employed to replace the expression involving $B_1\cos^2\theta_0$ in [6].

We now turn to the permeation equation. It is clear that $\dot{\Phi} = 0$ for $\mathbf{v}$ given by (2.24) and so the permeation equation (2.13) becomes $J_{i,i} = 0$, assuming $\lambda_\mathrm{p} > 0$. Notice that $\partial|\nabla\Phi|/\partial\Phi_{,i} = a_i$. For the energy density given by (2.19), $\mathbf{J}$ defined by (2.7) is

$$J_i = -B_0(|\nabla\Phi| + (\mathbf{n}\cdot\mathbf{a}) - 2)a_i + \frac{1}{|\nabla\Phi|}[K(\nabla\cdot\mathbf{a})_{,i} - B_0(|\nabla\Phi| + (\mathbf{n}\cdot\mathbf{a}) - 2)n_i + B_1(\mathbf{n}\cdot\mathbf{a})n_i - K(\nabla\cdot\mathbf{a})_{,k}a_i a_k + B_0(|\nabla\Phi| + (\mathbf{n}\cdot\mathbf{a}) - 2)(\mathbf{n}\cdot\mathbf{a})a_i - B_1(\mathbf{n}\cdot\mathbf{a})^2 a_i]. \tag{3.11}$$

Inserting the approximations (3.2) and (3.3) into this expression, linearizing appropriately and then taking its divergence and setting it equal to zero gives the permeation equation

$$J_{i,i} = 0, \tag{3.12}$$

where

$$J_{i,i} = B_0\hat{\theta}_{,z}\sin\theta_0 + B_1\hat{\phi}_{,y}\sin\theta_0\cos\theta_0 + B_0\hat{\phi}_{,y}\sin\theta_0(1-\cos\theta_0) - B_0\hat{u}_{,yy}(1-\cos\theta_0)^2 + B_1\hat{u}_{,yy}\cos^2\theta_0 + B_0\hat{u}_{,zz} - K\hat{u}_{,yyyy}. \tag{3.13}$$

The three equations (3.8), (3.10) and (3.12) are the governing equations for the minimal set of variables. These equations are very similar to those in [6], with some minor differences: the results in [6] were derived from an alternative linearized version of a different theory for the dynamics of SmA. It is remarkable that the equations here only differ in three terms, all nonlinear in θ_0, namely the B_0 term in (3.8) and the B_0 terms in the third and fourth expressions in (3.13); in fact, the governing equations derived here coincide precisely with those in [6] for small values of θ_0. We consider periodic ansatzes for the perturbed variables $\hat{\theta}$, $\hat{\phi}$ and $\hat{u}$ of the form

$$\{\hat{\theta}, \hat{\phi}, \hat{u}\} = \{A_\theta, A_\phi, A_u\}\,\mathrm{e}^{\mathrm{i}(qy + q_z z)}, \tag{3.14}$$

where A_θ, A_ϕ and A_u are small constants which govern the amplitude of the corresponding perturbations; q and q_z are wavenumbers in the x and z directions, respectively (it will be clear from the context that the notation in (3.14) will not be confused with any indices used in Cartesian notation). Inserting (3.14) into the aforementioned governing equations gives a system of linear equations in the amplitudes, namely

$$\frac{\mathrm{i}q}{\gamma_1}[B_1 + B_0(\sec\theta_0 - 1)]A_u + \frac{1}{2}k(1+\lambda)A_\phi = 0, \tag{3.15}$$

$$\left[\frac{\sin^2\theta_0}{\gamma_1}(B_0 - B_1) + k\lambda\sin\theta_0\cos\theta_0 + \frac{k}{2}(1+\lambda)\cot\theta_0\right]A_\theta + \frac{\mathrm{i}q_z}{\gamma_1}B_0\sin\theta_0 A_u = 0, \tag{3.16}$$

$$\mathrm{i}q_z B_0\sin\theta_0 A_\theta + \mathrm{i}q\sin\theta_0[B_1\cos\theta_0 + B_0(1-\cos\theta_0)]A_\phi - [Kq^4 - B_0q^2(1-\cos\theta_0)^2 + B_1q^2\cos^2\theta_0 + B_0q_z^2]A_u = 0. \tag{3.17}$$

We can write these equations as a matrix system with constant coefficients in the form

$$A\mathbf{x} = \mathbf{0}, \tag{3.18}$$

where A is the appropriate constant coefficient matrix and $\mathbf{x} = [A_\theta, A_\phi, A_u]^\mathrm{T}$. A non-zero solution requires $\det(A) = 0$. For a given set of material parameters, including a presumed wavenumber q_z, $\det(A)$ is easily seen to be real, in which case $\det(A) = 0$ determines a curve in the $q\theta_0$ plane. The minimum value for θ_0 on this curve determines the actual critical angle θ_c at which a non-zero perturbation will be available. This critical angle is directly related to a critical shear rate k_c that can be calculated from the relation (2.28). There will be a corresponding value for q at θ_c, which will be denoted by q_c. It is at the critical shear rate k_c that the spatially homogeneous

state given by (2.22)–(2.24) and (2.28) will then have a director tilt at θ_c and begin to exhibit the onset of an undulation of the smectic layers along the y direction with wavelength given by $2\pi/q_c$. Calculations for the identification of θ_c and q_c will be made in section 4 below after we have derived a set of model equations for the same problem with coupling to flow included. The dependence of these critical parameters upon various material parameters will be investigated numerically. Calculations will be based on a set of representative values listed in table 1 and the numerical results for the minimal set of variables will be presented in parallel with those for a full set of variables. We will then be in a position to compare the results obtained from the minimal set with those obtained from a set of variables that include coupling to the velocity.

3.2. Case 2: coupling to the velocity

Having examined the simple shear problem without coupling to the velocity and determined a set of three equations for the minimal set of variables in case 1, we now turn our attention to the coupling with the velocity. This will enable us to make a comparison between the results that incorporate a perturbed flow with those that do not. As before, the form of the perturbations will be given by (3.1), the key difference now being the introduction of a perturbation to the shear flow (2.24) by considering

$$\mathbf{v} = (kz, 0, 0) + (v_x(y,z), v_y(y,z), v_z(y,z)), \tag{3.19}$$

where v_x, v_y and v_z are small. There will be seven governing equations: one from the incompressibility condition, two from the angular momentum equations, one from the permeation equation and three from the linear momentum equations.

The incompressibility condition (2.3) results in the equation

$$v_{y,y} + v_{z,z} = 0. \tag{3.20}$$

The equations arising from angular momentum are again given by equation (3.6), except that in this case $\mathbf{a}$ and $\mathbf{n}$ are given by (3.3) and the $\tilde{g}_i$ contributions are given via (2.21), (3.1), (3.3) and (3.19) by

$$\tilde{g}_1 = \tfrac{1}{2}(\gamma_1 - \gamma_2)[(k + v_{x,z})\cos\theta_0 - k\hat{\theta}\sin\theta_0], \tag{3.21}$$

$$\tilde{g}_2 = -\tfrac{1}{2}(\gamma_1 + \gamma_2)(v_{x,y}\sin\theta_0 + v_{z,y}\cos\theta_0) + \tfrac{1}{2}(\gamma_1 - \gamma_2)v_{y,z}\cos\theta_0, \tag{3.22}$$

$$\tilde{g}_3 = -\tfrac{1}{2}(\gamma_1 + \gamma_2)[(k + v_{x,z})\sin\theta_0 + k\hat{\theta}\cos\theta_0] - \gamma_2 v_{z,z}\cos\theta_0. \tag{3.23}$$

Notice that here $\mathbf{n}\cdot\mathbf{a} = \cos\theta_0 - \hat{\theta}\sin\theta_0$, as in the first case above. As before, the Lagrange multiplier μ in this case can be determined from the $i = 1$ equation in (3.6) to reveal that, to first order in the variables,

$$\mu = \tfrac{1}{2}(\gamma_1 - \gamma_2)[(k + v_{x,z})\cot\theta_0 - k\,\hat{\theta}\,\mathrm{cosec}^2\theta_0]. \tag{3.24}$$

Putting this value for μ into equation (3.6) and using (3.3), (3.22) and (3.23) gives, for the $i = 2$ equation,

$$[B_0(\sec\theta_0 - 1) + B_1]\frac{\hat{u}_y}{\gamma_1} + \frac{1}{2}(1-\lambda)(v_{z,y} + v_{x,y}\tan\theta_0) + \tfrac{1}{2}(1+\lambda)(k\hat{\phi} - v_{y,z}) = 0, \tag{3.25}$$

while the $i = 3$ equation, after an appropriate use of (2.28) to replace the $B_1\cos^2\theta_0$ contribution, gives

$$\hat{\theta}\left[\frac{2}{\gamma_1}(B_0 - B_1)\sin^2\theta_0 + 2k\lambda\cos\theta_0\sin\theta_0 + k(1+\lambda)\cot\theta_0\right] + 2\frac{B_0}{\gamma_1}\hat{u}_{,z}\sin\theta_0 - v_{x,z}[1 + \lambda\cos(2\theta_0)] + 2\lambda v_{z,z}\cos\theta_0\sin\theta_0 = 0. \tag{3.26}$$

For the form of Φ given in (3.1), $\dot{\Phi} = v_z$ to first order. The divergence of $\mathbf{J}$ remains as stated in equation (3.13), because it does not contain contributions from the flow. Thus the linearized permeation equation (2.13) is

$$v_z + \lambda_p J_{i,i} = 0, \tag{3.27}$$

where $J_{i,i}$ is given by (3.13).

It only remains to consider the linear momentum equations (2.6) in the absence of body forces. We shall assume that $\tilde{p}$ is a function of y and z only, in common with the assumed dependences for the other variables in the problem. The three equations in (2.6) are then, to first order,

$$\rho v_z k = \tilde{t}_{1j,j}, \tag{3.28}$$

$$0 = -\tilde{p}_{,y} + \tilde{g}_j n_{j,2} + \tilde{t}_{2j,j}, \tag{3.29}$$

$$0 = -\tilde{p}_{,z} + \tilde{g}_j n_{j,3} + \tilde{t}_{3j,j} + J_{i,i}, \tag{3.30}$$

where the components of $\tilde{t}_{ij}$ are given by (2.20), $J_{i,i}$ is given by (3.13) and the $\tilde{g}_i$ are as stated in (3.21) to (3.23); it follows that

$$\begin{aligned} \tilde{g}_j n_{j,2} &= \tfrac{1}{2}k[\gamma_1 - \gamma_2\cos(2\theta_0)]\hat{\theta}_{,y}, \\ \tilde{g}_j n_{j,3} &= \tfrac{1}{2}k[\gamma_1 - \gamma_2\cos(2\theta_0)]\hat{\theta}_{,z}, \end{aligned} \tag{3.31}$$

and we note for calculations that, when linearized in the variables, $\dot{\mathbf{n}} = \mathbf{0}$ and

$$N_1 = \tfrac{1}{2}[k\hat{\theta}\sin\theta_0 - (k + v_{x,z})\cos\theta_0], \tag{3.32}$$

$$N_2 = \tfrac{1}{2}[v_{x,y}\sin\theta_0 + (v_{z,y} - v_{y,z})\cos\theta_0], \tag{3.33}$$

$$N_3 = \tfrac{1}{2}[k\hat{\theta}\cos\theta_0 + (k + v_{x,z})\sin\theta_0]. \tag{3.34}$$

The seven governing equations for our problem are therefore given by equations (3.20) and (3.25)–(3.30).

We now progress as in the first case by introducing suitable ansatzes and set

$$\{\hat{\theta}, \hat{\phi}, \hat{u}, v_x, v_y, v_z, \tilde{p}\} = \{A_\theta, A_\phi, A_u, A_{v_x}, A_{v_y}, A_{v_z}, A_p\} \times e^{i(qy + q_z z)}, \tag{3.35}$$

where A_θ, A_ϕ, A_u, A_{v_x}, A_{v_y}, A_{v_z} and A_p are small amplitudes, with the aim of constructing a matrix system of seven equations in these unknown constants. Inserting (3.35) into the relevant seven equations (3.20) and (3.25)–(3.30) and linearizing gives (after some straightforward calculations), respectively:

$$qA_{v_y} + q_z A_{v_z} = 0, \tag{3.36}$$

$$k(1+\lambda)A_\phi + 2\frac{iq}{\gamma_1}[B_0(\sec\theta_0 - 1) + B_1]A_u + iq(1-\lambda) \times \tan\theta_0 A_{v_x} - iq_z(1+\lambda)A_{v_y} + iq(1-\lambda)A_{v_z} = 0, \tag{3.37}$$

$$\left[\frac{2}{\gamma_1}(B_0 - B_1)\sin^2\theta_0 + 2k\lambda\cos\theta_0\sin\theta_0 + k(1+\lambda)\cot\theta_0\right]A_\theta + 2\mathrm{i}q_z\frac{B_0}{\gamma_1}\sin\theta_0 A_u - \mathrm{i}q_z[1+\lambda\cos(2\theta_0)]A_{v_x} + 2\mathrm{i}q_z\lambda\cos\theta_0\sin\theta_0 A_{v_z} = 0. \quad (3.38)$$

$$\mathrm{i}q_z\lambda_\mathrm{p}B_0\sin\theta_0 A_\theta + \mathrm{i}q\lambda_\mathrm{p}\sin\theta_0[B_1\cos\theta_0 + B_0(1-\cos\theta_0)]A_\phi - \lambda_\mathrm{p}[Kq^4 - B_0q^2(1-\cos\theta_0)^2 + B_1q^2\cos^2\theta_0 + B_0q_z^2]A_u + A_{v_z} = 0, \quad (3.39)$$

$$\begin{aligned}&ki q_z[2\gamma_2\sin(2\theta_0) + \alpha_1\sin(4\theta_0)]A_\theta \\ &+ kiq\sin\theta_0\cos\theta_0[\alpha_5 - \alpha_2 + 2\alpha_1\sin^2\theta_0]A_\phi \\ &+ \tau_2kq^2A_u - [(\alpha_2+2\alpha_3)(q^2+q_z^2)\sin^2\theta_0 \\ &- \alpha_2q_z^2\cos^2\theta_0 + \tau_2q_z^2 + \alpha_4(q^2+q_z^2) \\ &+ 2\alpha_1q_z^2\sin^2\theta_0\cos^2\theta_0 + \alpha_5(q_z^2 + q^2\sin^2\theta_0)]A_{v_x} \\ &- qq_z(\alpha_2+\alpha_5)\sin\theta_0\cos\theta_0A_{v_y} \\ &- (2\rho k + [(2\alpha_3+\alpha_2+\alpha_5)q^2 \\ &+ 2(\gamma_2+\alpha_5+\alpha_1\cos^2\theta_0)q_z^2]\sin\theta_0\cos\theta_0)A_{v_z} = 0,\end{aligned} \quad (3.40)$$

$$\begin{aligned}&kiq[\gamma_1 - \gamma_2\cos(2\theta_0)]A_\theta \\ &+ kiq_z(2\alpha_1\cos^2\theta_0 + \alpha_2 + 2\alpha_3 + \alpha_5)\sin^2\theta_0A_\phi \\ &- (\alpha_2+\alpha_5)qq_z\sin\theta_0\cos\theta_0A_{v_x} \\ &+ [q_z^2((\alpha_2-\alpha_5)\cos^2\theta_0 - \tau_2 - \alpha_4) - 2\alpha_4q^2]A_{v_y} \\ &- qq_z[(\alpha_2+\alpha_5)\cos^2\theta_0 + \tau_2 + \alpha_4]A_{v_z} - 2iqA_p = 0,\end{aligned} \quad (3.41)$$

$$\begin{aligned}&\mathrm{i}q_z[2B_0\sin\theta_0 + k(\gamma_1 + (\gamma_2+2\alpha_5)\cos(2\theta_0)) \\ &+ 2k\alpha_1\cos^2\theta_0(4\cos^2\theta_0 - 3)]A_\theta \\ &+ \mathrm{i}q\sin\theta_0[2B_1\cos\theta_0 + 2B_0(1-\cos\theta_0) \\ &+ k(2\alpha_1\cos^2\theta_0 + \alpha_2 + \alpha_5)\sin\theta_0]A_\phi \\ &- 2[B_1q^2\cos^2\theta_0 - B_0q^2(1-\cos\theta_0)^2 \\ &+ B_0q_z^2 + Kq^4]A_u - \sin\theta_0\cos\theta_0 \\ &\times[2(\alpha_1\cos^2\theta_0 + \gamma_2 + \alpha_5)q_z^2 \\ &+ (\alpha_2 + 2\alpha_3 + \alpha_5)q^2]A_{v_x} \\ &- qq_z[(\alpha_2+\alpha_5)\cos^2\theta_0 + \alpha_4 + \tau_2]A_{v_y} \\ &- [(\alpha_2+2\alpha_3)q^2\cos^2\theta_0 + \alpha_4(q^2+2q_z^2) \\ &+ 2(\alpha_1\cos^4\theta_0 + \tau_1)q_z^2 + (\alpha_5\cos^2\theta_0 + \tau_2) \\ &\times(q^2+4q_z^2) + 2\gamma_2q_z^2\cos^2\theta_0]A_{v_z} - 2\mathrm{i}q_zA_p = 0.\end{aligned} \quad (3.42)$$

As in case 1, we can write equations (3.36)–(3.42) as a matrix system of the form given in (3.18) where, in this case, A is the relevant matrix of constant coefficients and $\mathbf{x} = [A_\theta, A_\phi, A_u, A_{v_x}, A_{v_y}, A_{v_z}, A_p]^\mathrm{T}$. The comments concerning the minimal set of variables after equation (3.18) are equally valid here: we need to determine the minimum q_c and θ_c that can be found from the requirement for non-zero solutions that $\det(A) = 0$, for a given set of material parameters. In the minimal set case we have a 3×3 determinant to consider while in the coupled flow case it will be a 7×7 determinant.

4. Solutions

The main results will involve the identification of a critical tilt angle at the onset of an instability to the spatially homogeneous state (2.28) that is directly related to the applied shear rate k, as has been discussed above in section 2.3 for figure 2. The two sets of equations given by (3.15)–(3.17), for the minimal case without coupling to the velocity field, and (3.36)–(3.42), for the case with coupling to flow, will be used to produce graphs that highlight the dependence of the critical parameters upon various material parameters for the problem outlined above. The parameters and typical values used when solving our equations are stated in table 1. We have chosen a common value for the sample depth and set $d = 10^{-5}$ m. The elastic constant K and viscosities α_1 to α_5 are based on representative values for the nematic liquid crystal 5CB while B_0 is a typical value for the smectic layer compression constant [2]. The coupling constant B_1 has been chosen in line with the estimates by Ribotta and Durand [3] ($B_1 \lesssim B_0$) for SmA and the permeation constant λ_p has been estimated by Kléman and Lavrentovich [18 p 328] (early measurements for λ_p by Chan and Webb [21] for lamellar bilayers were substantially smaller than this (10^{-33} m^2 Pa^{-1} s^{-1}): the value quoted in table 1 is in agreement with the experimental evidence reported by Krüger [22], as considered in [18]).

As discussed above, each of the aforementioned systems of linear equations can be written as a matrix system with constant coefficients in the form $A\mathbf{x} = \mathbf{0}$, where A is the appropriate coefficient matrix and $\mathbf{x} = [A_\theta, A_\phi, A_u]^\mathrm{T}$ for the minimal variables case and $\mathbf{x} = [A_\theta, A_\phi, A_u, A_{v_x}, A_{v_y}, A_{v_z}, A_p]^\mathrm{T}$ for the case with perturbation to the velocity field included. Each system has non-zero solutions if and only if $\det(A) = 0$. In each case, this requirement determines a curve in the $q\theta_0$ plane whenever the parameters from table 1 are inserted into the components of the matrix A; recall that θ_0 can always be related back to the applied shear rate k via the relation (2.28). The resulting curves for $\det(A) = 0$ are shown in figure 3 for a range of values in q and θ_0: the solid line represents the curve for the minimal set of three variables while the dashed line is that for the case with the full set of seven variables when coupling of the perturbations to the velocity field is included. These curves and subsequent results have been obtained using data calculated from the software package Maple [23]. From the curves in figure 3 it is readily seen that there is a minimum value of θ_0, written as the critical value θ_c, which occurs at a corresponding critical wavenumber $q = q_\mathrm{c}$. At the onset of the instability to the stationary state the director will tilt at an angle θ_c and the layers will exhibit a periodic structure in the y direction with wavelength $2\pi/q_\mathrm{c}$. The corresponding critical shear rate k_c at which the onset of the instability occurs can be determined from (2.28) or the graph plotted in figure 2. In this instance we have

$$\begin{aligned}&\text{minimal set:} \quad q_\mathrm{c} = 3.6431\times10^7\ \mathrm{m}^{-1}, \\ &\theta_\mathrm{c} = 0.0174\ \mathrm{rad}, \quad k_\mathrm{c} = 8.5753\times10^6\ \mathrm{s}^{-1},\end{aligned} \quad (4.1)$$

$$\begin{aligned}&\text{coupling to velocity:} \quad q_\mathrm{c} = 3.6408\times10^7\ \mathrm{m}^{-1}, \\ &\theta_\mathrm{c} = 0.0164\ \mathrm{rad}, \quad k_\mathrm{c} = 8.0821\times10^6\ \mathrm{s}^{-1}.\end{aligned} \quad (4.2)$$

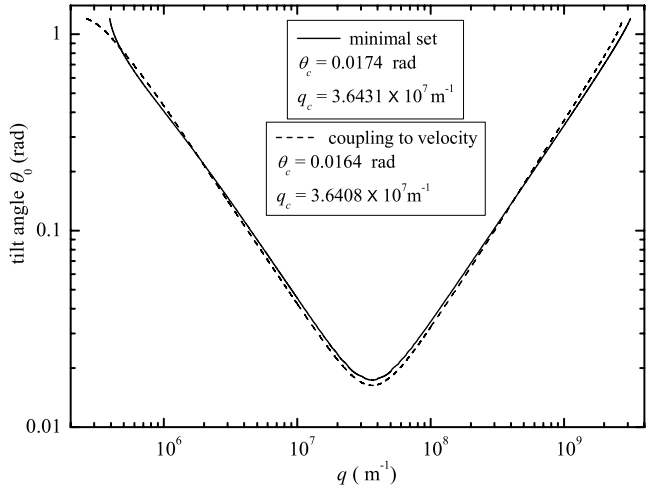

Figure 3. Log–log plots of the curves $\det(A(q, \theta_0)) = 0$ when the parameters from table 1 are inserted into the coefficient matrix A. The solid line represents the curve for the minimal set of variables while the dashed line is for the case when coupling to the velocity field is included. The critical tilt angle for the director, θ_c, is the minimum value of θ_0, achieved at a corresponding critical wavenumber q_c.

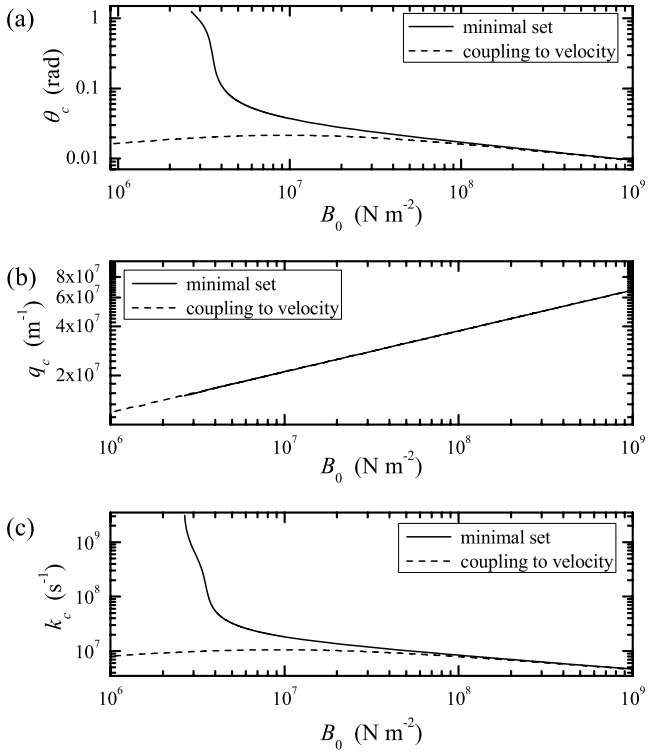

Figure 4. (a) Plots of θ_c as a function of B_0 plotted on a log–log graph. For high magnitudes of B_0 the curves almost coincide. The curves separate for low values of B_0. (b) Plots of the critical wavenumber q_c as a function of B_0. The curves are virtually coincident. (c) The critical shear rate k_c as a function of B_0, calculated via (3.28) and the data for θ_c in (a). All remaining material parameters have been set to those stated in table 1.

It is seen that coupling to the velocity does slightly reduce the values of q_c, θ_c and k_c; the influence of flow, in this particular example, does not dramatically change the critical values. We remark that high shear rates such as these are not uncommon in shear flow experiments in molecular dynamics models [24]. Figure 3 essentially shows how to obtain the critical values q_c and θ_c for a given set of material parameters. It is this procedure that we now adopt as we investigate how the values of θ_c, q_c and k_c change as various parameters vary: as one particular parameter varies, we can calculate the corresponding critical values.

In figure 4 we suppose that the parameter values are as stated in table 1 except for B_0 and explore the effect that varying B_0 has on the critical tilt angle of the director, the critical wavenumber and the critical shear rate, plotted on log–log graphs. The dependence of θ_c upon the layer compression constant B_0 is shown in figure 4(a). This figure shows quite different results for small values of B_0 which depend on whether or not coupling to the velocity field is included. The influence of flow is seen to be substantial when B_0 is relatively smaller than B_1 and the difference between the results for the minimal and full sets of variables is greatest when B_0 is small. However, as B_0 approaches the value of $B_1 = 4 \times 10^7$ N m^{-2} the results begin to coincide. Despite $B_1 \lesssim B_0$ being a common assumption [3], if it is, nevertheless, anticipated that B_0 is smaller than B_1 then coupling of the perturbations to the velocity may be required for a more accurate model. The results in figure 4(b) show the corresponding dependence of q_c upon B_0. The difference between the values of q_c calculated with and without coupling to the flow are negligible. It may be of interest to note from figure 4(b) that the linear plots show $q_c(B_0)$ satisfies a power law relation given by, in this particular case, $q_c = aB_0^b$ where $a \approx 3.74 \times 10^5$ and $b \approx 0.25$. The origin of this power law behaviour is discussed in more generality in section 5 via the results in equation (5.1), which lead to the approximation stated in equation (5.3) that happens to be in line with the above numerically derived result. The corresponding critical shear rate k_c, shown in figure 4(c), has been calculated from the data in figure 4(a) for θ_c and the expression for the shear rate given by equation (3.28). Recall that the onset of the instability will occur at the critical shear rate k_c. The critical tilt angle and the critical shear rate are seen to be generally reduced in magnitude if coupling to the velocity is included compared to the case for the minimal set of variables.

The dependence of θ_c and q_c upon B_1 can be examined similarly when the remaining parameters are fixed at the values stated in table 1. The results are shown in figure 5. In figure 5(a), the effect upon θ_c of coupling to the velocity becomes more prominent as B_1 increases: in general, θ_c decreases as B_1 increases when coupling to the velocity is included, in contrast to a slight increase in θ_c for the minimal set of material parameters. The corresponding values for q_c are displayed in figure 5(b). For both sets of variables, the curves for q_c are close for $B_1 \lesssim 10^7$ N m^{-2}, and begin to separate for values of B_1 greater than this; when coupled to the velocity for large values of B_1, q_c is lower than that obtained for the minimal set of variables. The horizontal axes in figures 5(a) and (b) are on a log scale. It is seen in figure 5(c) (with unscaled axes) that the critical shear rate k_c is linearly increasing with B_1

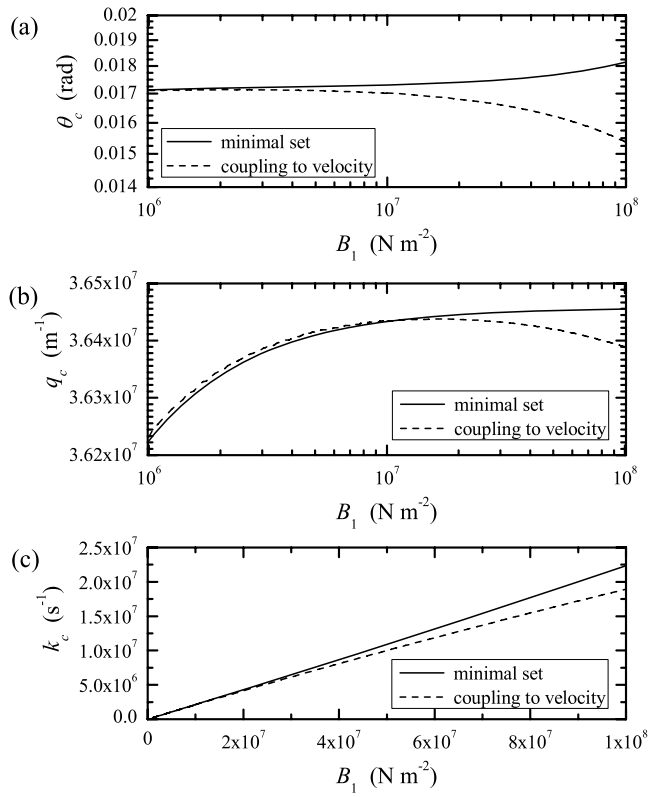

Figure 5. The horizontal axes in (a) and (b) are on a log scale. (a) Plots of θ_c as a function of B_1. The curves separate for high values of B_1. (b) Plots of the critical wavenumber q_c as a function of B_1. The curves separate as B_1 increases. (c) The critical shear rate k_c, calculated via (3.28) and the data for θ_c in (a). The remaining material parameters are as stated in table 1.

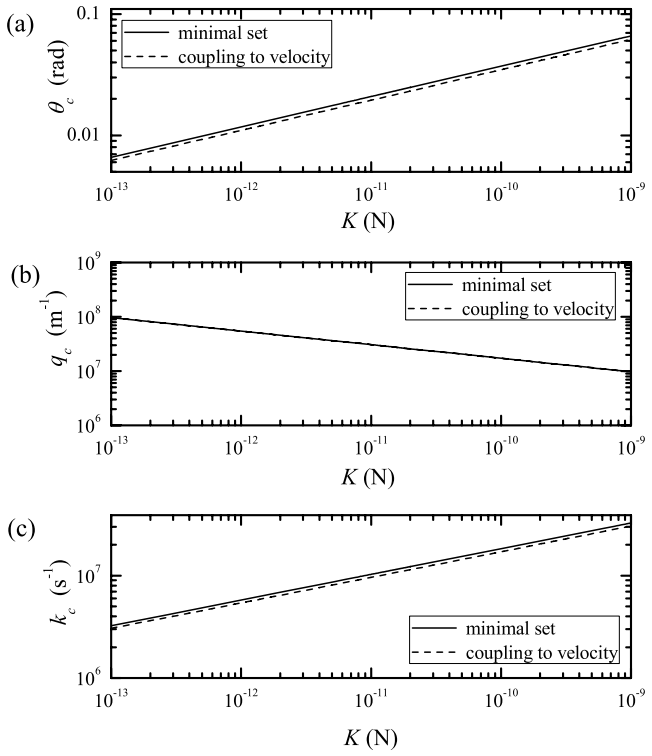

Figure 6. (a) Plots of θ_c as a function of K plotted on a log–log graph. (b) Plots of q_c as a function of K. (c) The dependence upon K of the critical shear rate k_c. The remaining material parameters are as stated in table 1.

for both the minimal and full sets of variables. Moreover, the critical shear rate when coupling to the velocity is included is always lower than the corresponding shear rate for the minimal set. It is known from the approximation in (2.29) that, for small angles θ_c, k_c is approximately linear in B_1. For the data given by table 1, the linear dependences can be approximated from the numerical data to find that $k_c = a + bB_1$ where $a \approx -8.46 \times 10^4$, $b \approx 0.222$ for the minimal set of variables and $a \approx 5.16 \times 10^5$, $b \approx 0.187$ when coupling to the velocity is included. The behaviour of k_c here is distinctly different from that shown in figure 4(c) for varying B_0.

By a similar approach we now consider the dependence of the critical values θ_c, q_c and k_c on the bending modulus of the layers K while the other material parameters remain as given in table 1. From figure 6(a), it is clear that, as K increases, the critical tilt angle θ_c of the director increases for both sets of variables. Although both cases demonstrate linear behaviour on log–log graphs, the inclusion of flow leads to a slightly lower tilt angle in comparison to the minimal variables case. It is also seen in figure 6(b) that, as K increases, the critical wavenumber q_c decreases with the curves for both sets of variables being almost indistinguishable. Figure 6(c) shows that the critical shear rate k_c is linearly increasing with K (on a log–log graph) for both the minimal and full sets of variables; the value of k_c, obtained from (3.28) and the data for θ_c in figure 6(a), is always slightly lower than that obtained

Table 2. The approximate power law behaviour for the critical parameters shown in figure 6. The remaining material constants are as stated in table 1.

	Minimal set		Coupling to velocity	
	a	b	a	b
$\theta_c = aK^b$	11.6961	0.2498	10.9595	0.2500
$q_c = aK^b$	5.4359×10^4	−0.2501	5.5698×10^4	−0.2491
$k_c = aK^b$	5.9328×10^9	0.2510	5.5184×10^9	0.2508

for the minimal set of variables when coupling to the velocity is included. All of the plots in figure 6 are linear on log–log graphs and so they can be approximated by power laws. Table 2 shows the results for these approximations, obtained via the software package Origin 8 [25]. The origin of these power laws can be determined under the assumption that θ_c is small at criticality. The general approximations discussed in section 5 below at equation (5.1) reveal the material parameter dependences of θ_c, q_c and k_c. The results stated in (5.2) are in keeping with those presented in table 2.

The permeation constant, λ_p, only has an influence when coupling to the velocity is included. Graphs of the dependence of θ_c, q_c and k_c on λ_p are shown in figure 7, where the horizontal axes are on a log scale. Although we have set $\lambda_p = 10^{-16}$ m^2 Pa^{-1} s^{-1} for all of the preceding calculations, the three key critical parameters are most sensitive to change when λ_p varies around 10^{-14} m^2 Pa^{-1} s^{-1}. As λ_p increases, both θ_c and k_c increase as shown in figures 7(a) and (c) while the critical wavenumber at the onset of the instability

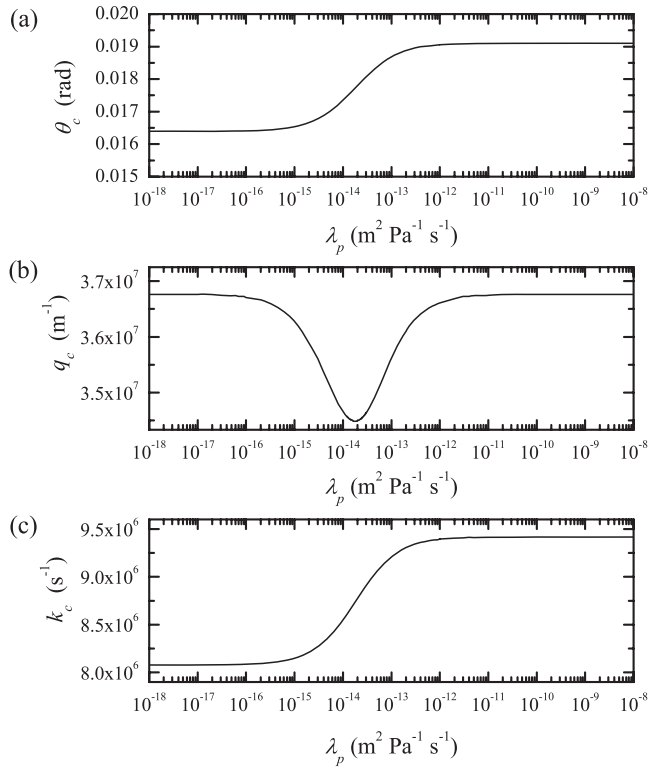

Figure 7. The horizontal axes are on a log scale. (a) A plot of θ_c as a function of λ_p with the other material parameters as stated in table 1. (b) q_c as a function of λ_p. (c) The dependence on λ_p of the critical shear rate k_c for the onset of instability. The remaining material parameters are as stated in table 1.

remains constant close to 3.64×10^7 m^{-1} except over the region approximately given by 5×10^{-17} m^2 Pa^{-1} s^{-1} $< \lambda_p <$ 5×10^{-11} m^2 Pa^{-1} s^{-1}; this region also happens to be where θ_c and k_c vary most as λ_p changes. For the two extreme possibilities of small and large magnitude permeation, θ_c, q_c and k_c are close to constant values: for λ_p small and the other material parameters given in table 1, $\theta_c \approx 0.0164$ rad and $k_c \approx 8.0784 \times 10^6$ s^{-1}, and for very much large values of λ_p, $\theta_c \approx 0.0191$ rad and $k_c \approx 9.4163 \times 10^6$ s^{-1}. As mentioned in the opening paragraph to this section, there are widely different values reported for λ_p for different lamellar systems and that it may be very much smaller than the range indicated here for lamellar bilayers [21]. Nevertheless, the range of values for λ_p used here is known to be within those reported and estimated for SmA liquid crystals [1, 18].

5. Conclusions and discussion

The decoupling of the director **n** from the layer normal **a** has been highly significant in motivating the work contained in this paper. The common Oseen constraint for smectics, that is, $\nabla \times \mathbf{a} = \mathbf{0}$, has also not been imposed as a necessary requirement in the modelling of the dynamics of SmA liquid crystals. We have examined the onset of an instability induced by a simple shear in a planar aligned sample of SmA and the prime concern has been the identification of critical values at the start of the instability. For given material parameters, the critical shear rate, k_c, at which the beginning of the instability occurs, has been determined from the corresponding critical tilt angle, θ_c, of the director; a general technique for finding the associated wavenumber, q_c, has also been developed. The results presented above have been based on two sets of model dynamic equations that consider the perturbation to a homogeneous state given by equation (2.22) and have been derived as special cases of a more general theory [12]. A useful nonlinear relation between the shear rate and the director tilt angle was identified in equation (2.28) for a spatially homogeneous state. A linear approximation to this relation was given in (2.29) and a comparison between the nonlinear and linear versions was made in figure 2. When a critical tilt angle has been identified then this relation enables a corresponding critical shear rate to be evaluated directly. It also means that k_c can be replaced in terms of θ_c and vice versa at criticality. The first set of equations is based on a minimal set of three perturbation variables, namely $\hat{\theta}$, $\hat{\phi}$ and $\hat{u}$ as given by (3.14). The second set consists of seven perturbation variables, labelled $\hat{\theta}$, $\hat{\phi}$, $\hat{u}$, v_x, v_y, v_z and $\tilde{p}$, as introduced in (3.35). The minimal set ignored coupling of the perturbations to the velocity while the second set of full variables allowed a coupling to the velocity; considering both sets of variables enables a comparison to be made so that the influence of flow can be investigated. In many simplified dynamic problems, any possible coupling to the velocity is often neglected and therefore the qualitative results presented here will, to some extent, provide a guide as to whether or not it is reasonable to ignore coupling to the velocity in approximations to more complex problems, especially when some of the material parameters are known from experimental data.

The two sets of dynamic equations led to linearized systems in the unknown small amplitudes of the perturbation variables and the requirement for non-zero solutions forced the associated determinant of the matrix of coefficients to be zero, which is the criterion discussed in section 3 for the determination of the critical parameters via determinant curves such as those shown in figure 3. The techniques for obtaining critical values for θ_c and k_c from such curves were discussed in detail and exploited in section 4. It was first noted in section 2.3 that the results for a spatially homogeneous state under an imposed simple shear were in accord with those obtained from an alternative dynamic theory for SmA [6]. Furthermore, the dynamic equations given by (3.8), (3.10) and (3.12) for the minimal set of variables are, when linearized, almost coincident with those in [6] and are actually identical for small values of θ_0, as highlighted after equation (3.13). Nevertheless, when coupling to the velocity was included in section 3.2 the dynamic equations differed from those in [6] because of the form of the viscous terms introduced at equations (2.20) and (2.21). Further, a non-dimensionalized set of equations was used in [6] whereas we have retained dimensions so that a direct comparison with experimental data can be made. The reduced number of viscosities in expressions (2.20) and (2.21) have been selected because they are considered to be representative of the minimum collection of viscosity coefficients that can be adopted in order to

incorporate the basic nematic-like and smectic-like behaviour, largely motivated by the SmA model reviewed in [1]. The reader is referred to the paper by Osipov *et al* [26] for a more detailed general discussion of viscosity coefficients in smectics.

The main results have been presented in section 4 for the typical material parameters listed in table 1. These tabulated parameters are representative values which allow qualitative and quantitative results to be generated. Figure 4 shows the dependence of the critical values as the smectic layer compression constant B_0 varies while other parameters remain fixed as given in table 1. The differences between the minimal set solutions and those when coupling to flow is included are most evident for small magnitudes of B_0. When the layer compression constant is small then the influence of flow is substantial compared to the situation in the presumed absence of flow and therefore these results indicate that the inclusion of flow will generally be of importance and cannot be neglected when searching for critical shear rates k_c and tilt angles θ_c when B_0 is relatively smaller than the director and layer normal coupling constant B_1. It remains to be seen how important these observations are, especially given the early conjecture by Ribotta and Durand [3], mentioned in section 4, that the magnitude of B_1 may well be less than that of B_0 for SmA. This then led naturally to an investigation of the dependence of the critical values on B_1 with the results shown in figure 5. For B_1 relatively smaller than B_0 (which was set at 8.95×10^7 N m^{-2} in the figure) the solutions for the minimal set of variables are very close to those for the full set of variables. Therefore if $B_1 \lesssim B_0$ then using the minimal set of variables may be sufficient in modelling critical shear effects. The discrepancies between the curves shown in figure 5 are more pronounced as B_1 increases; all three critical values obtained from the minimal set are reduced in magnitude when coupling to the velocity is included for high values of B_1.

The results in figure 6 show the critical values as functions of the elastic constant K, the other parameters being fixed at the values in table 1. The apparent linear dependences on K shown on log–log graphs allowed us to approximate θ_c, q_c and k_c in terms of power laws; the numerical coefficients have been tabulated in table 2 where all the critical parameters are approximately proportional to K^b where b is negative for q_c and positive for both θ_c and k_c. These power laws may be quite general in form, in which case the sign of b is an important signature of the expected behaviour. It was also noted that when coupling to the velocity was included the values of θ_c and k_c in figures 6(a) and (c) were always slightly lower than those obtained for the minimal set of variables.

It is possible to determine the origin of the power laws that appear in figures 4(b) and 6. For example, if θ_0 is presumed small then the determinant of the matrix A that appears in (3.18) can be expanded to fourth order in θ_0 to obtain an expansion in the form $\det(A) = C_1\theta_0^2 + C_2\theta_0^4$, where C_1 and C_2 are dependent upon q and the remaining material parameters. This expansion has to be at least fourth order in order to eliminate $\theta_0 = \theta_c \equiv 0$ as the only solution; given the proximity of the results in the figures for the two coefficient matrices A that arise from the 'minimal set' and 'coupling to velocity' cases, we need only consider the minimal set to gain some insight into the problem. The aforementioned expansion can be solved explicitly for a unique positive solution θ_0. This expression for θ_0 can then be differentiated with respect to q in order to find the value $q = q_c$ at which θ_0 is minimized; the resultant q_c can then be expanded as a power series in any of the relevant material parameters such as B_0 and K. Once this has been accomplished, q_c may be inserted into the expression for θ_0 to obtain an approximation for θ_c. It is then also possible to obtain a corresponding expression for the critical shear rate k_c via the approximation (2.29). It is found that (recall that $\alpha_2 < 0$)

$$\theta_c \doteq \frac{2(B_0K)^{\frac{1}{4}}\sqrt{-\alpha_2 q_z}}{\sqrt{2B_1\alpha_3 - B_0\alpha_2}}, \qquad q_c \doteq \sqrt{q_z}\left(\frac{B_0}{K}\right)^{\frac{1}{4}}, \qquad k_c \doteq -\frac{B_1}{\alpha_2}\theta_c. \tag{5.1}$$

For the appropriate data in table 1, the relevant dependences on K can be calculated using (5.1) to reveal that

$$\theta_c = 11.76K^{\frac{1}{4}}, \qquad q_c = 5.45 \times 10^4 K^{-\frac{1}{4}}, \qquad k_c = 5.79 \times 10^9\, K^{\frac{1}{4}}. \tag{5.2}$$

These results are in reasonably close agreement with those presented in table 2 for the data presented in figure 6. The approximate formulae in (5.1) show the key parameters that influence the onset of a stationary instability to the spatially homogeneous state discussed in section 2.3. Similar calculations using (5.1) show that

$$q_c \doteq 3.75 \times 10^5 B_0^{\frac{1}{4}}, \tag{5.3}$$

again in accord with the data presented in figure 4(b) that was discussed in section 4.

The influence of permeation upon the critical values has been demonstrated in figure 7. This can only happen when there is coupling to the flow. A wide range of values for the permeation constant λ_p have been reported in the literature for different types of lamellar materials, ranging from 10^{-33} m^2 Pa^{-1} s^{-1} [21] to $\lambda_p = 10^{-16}$ m^2 Pa^{-1} s^{-1} [18, 22] and this has motivated the investigation into the role of λ_p as it varies. The results in figure 7 show that for high and low magnitudes of λ_p the critical values remain virtually constant. However, as seen in the figure, the system is most sensitive to variations in λ_p when it takes values in the range 5×10^{-17}–5×10^{-11} m^2 Pa^{-1} s^{-1}. Some experimental results by Lutti and Callaghan [27] on related systems of bilayers have indicated that permeation, which is a diffusion of material perpendicular to the smectic layers, may be reduced under the application of a weak shear. Moreover, the results in [27] for certain lamellar phases have demonstrated that smectic layer undulations can be suppressed by applying a weak shear. It may be possible to use the dynamic theory outlined in section 2.1 to model the dynamics of shear-induced undulations for shear rates above k_c and to compare theoretical predictions with the data presented in [27].

A more intricate nonlinear analysis will be worth investigating for shear rates that are very much greater than the critical shear rate k_c discussed above. The theoretical results by Wunenburger *et al* [28] on shear in SmA make some comparisons with experimental data for high shear rates. The theory and model discussed above may be developed and extended to look further into aspects of flow induced by high shear rates. Future work will also look at the inclusion of more viscosity coefficients, namely the coupling viscosities κ_1 to κ_6. A viscosity coefficient similar to κ_1 has appeared in dynamic theories for SmC liquid crystals (for example, the viscosity τ_1 introduced in [2, 16] and the coefficient γ_3 in [15]) and it is this particular viscosity that will be the focus of attention because it distinguishes the dynamic contribution $\tilde{g}_i$ from its nematic analogue [2]. The remaining viscosities κ_2 to κ_6 that appear in the viscous stress $\tilde{t}_{ij}$ in equation (2.9) have some analogous representations in SmC [2, 16] and reflect the coupling of **a** and **n** to the dynamics; for a brief discussion on related viscosities in SmC the reader is referred to [2, section 6.3.2]. The influence of such viscosities remains an area of interest for both SmC and SmA liquid crystals.

Acknowledgment

The authors are indebted to an anonymous referee for the invaluable suggestions that led to the expressions in equations (5.1)–(5.3).

References

[1] de Gennes P G and Prost J 1993 *The Physics of Liquid Crystals* 2nd edn (Oxford: Oxford University Press)
[2] Stewart I W 2004 *The Static and Dynamic Continuum Theory of Liquid Crystals* (London: Taylor and Francis)
[3] Ribotta R and Durand G 1977 *J. Physique* **38** 179–204
[4] Oswald P and Ben-Abraham S I 1982 *J. Physique* **43** 1193–7
[5] Auernhammer G K, Brand H R and Pleiner H 2000 *Rheol. Acta* **39** 215–22
[6] Auernhammer G K, Brand H R and Pleiner H 2002 *Phys. Rev.* E **66** 061707
[7] Auernhammer G K, Brand H R and Pleiner H 2005 *Phys. Rev.* E **71** 049901(E)
[8] Soddemann T, Auernhammer G K, Guo H, Dünweg B and Kremer K 2004 *Eur. Phys. J.* E **13** 141–51
[9] Stewart I W 2007 *J. Phys. A: Math. Theor.* **40** 5297–318
[10] Stewart F and Stewart I W 2007 *Mol. Cryst. Liq. Cryst.* **478** 23–32
[11] De Vita R and Stewart I W 2008 *J. Phys.: Condens. Matter* **20** 335101
[12] Stewart I W 2007 *Contin. Mech. Thermodyn.* **18** 343–60
[13] Oseen C W 1933 *Trans. Faraday Soc.* **29** 883–99
[14] E W 1997 *Arch. Ration. Mech. Anal.* **137** 159–75
[15] Sukumaran S and Ranganath G S 1998 *Phys. Rev.* E **57** 5597–608
[16] Leslie F M, Stewart I W and Nakagawa M 1991 *Mol. Cryst. Liq. Cryst.* **198** 443–54
[17] Shalaginov A N, Hazelwood L D and Sluckin T J 1999 *Phys. Rev.* E **60** 4199–209
[18] Kléman M and Lavrentovich O D 2003 *Soft Matter Physics: An Introduction* (New York: Springer)
[19] Helfrich W 1969 *Phys. Rev. Lett.* **23** 372–4
[20] Kramer L and Pesch W 2001 *Physical Properties of Liquid Crystals: Nematics* (*EMIS Datareviews Series No. 25*) ed D A Dunmur, A Fukuda and G R Luckhurst (London: The Institution of Electrical Engineers (INSPEC)) chapter 8.6 pp 441–54
[21] Chan W K and Webb W W 1981 *Phys. Rev. Lett.* **46** 603–6
[22] Krüger G J 1982 *Phys. Rep.* **82** 229–69
[23] Waterloo Maple Inc. 2007 *Maple 11* (Ontario: Waterloo Maple Inc.)
[24] Moore J D, Cui S T, Cochran H D and Cummings P T 2000 *J. Non-Newtonian Fluid Mech.* **93** 101–16
[25] OriginLab Corporation 2007 *Origin 8* (Northampton, MA: OriginLab Corp.)
[26] Osipov M A, Sluckin T J and Terentjev E M 1995 *Liq. Cryst.* **19** 197–205
[27] Lutti A and Callaghan P T 2006 *Phys. Rev.* E **73** 011710
[28] Wunenburger A S, Colin A, Colin T and Roux D 2000 *Eur. Phys. J.* E **2** 277–83